THE DISTRIBUTION WITH SIZE OF AGGREGATE SNOWFLAKES

By K. L. S. Gunn and J. S. Marshall

McGill University [1]

(Manuscript received 9 December 1957)

ABSTRACT

Average-size distributions for aggregate snowflakes are well represented above $D = 1$ mm by $N_D = N_0 e^{-\Lambda D}$ where D is the diameter of the water drop to which the aggregate would melt. This is the same equation that Marshall and Palmer (1948) reported for rain, but for rain $N_0 = 8.0 \times 10^3$ m^{-3} mm^{-1} and $\Lambda = 41\ R^{-0.21}$ while for snow $N_0 = 3.8 \times 10^3\ R^{-0.87}$ m^{-3} mm^{-1} and $\Lambda = 25.5\ R^{-0.48}$ where R is in millimeters of water per hour.

The sum of the sixth powers of the (melted) particle diameters in unit volume (Z), the mass of snow in unit volume (M), and the precipitation rate (R) are found to be related by $Z = 2000\ R^{2.0}$ and $M = 250\ R^{0.90}$; combining these two gives $Z = 9.57 \times 10^{-3}\ M^{2.2}$, with Z in mm^6 m^{-3}, M in mgm m^{-3} and R in mm hr^{-1} of water.

The relation $Z = 2000\ R^{2.0}$ is in good agreement with $Z = 2150\ R^{1.8}$, an average locus through recently reported Japanese data for aggregate flakes. The relation $Z = 200\ R^{1.6}$ for snow, published earlier by the present authors, is thought to be in error due to the method of sampling used at that time. Comparing standard rain and melted-snow distributions of the same R requires that there be considerable break-up of the larger particles when snow turns to rain at the melting level. Further, to explain the observed radar-signal increase from the rain over that from the snow, a considerable increase in R at or below the melting level is required.

1. Introduction

Over a period of some eight years at McGill, we have been sampling snow by various methods. The measurements of terminal speed of aggregate flakes reported by Langleben (1954) make possible the conversion of a distribution on a horizontal surface to the corresponding distribution in space. This paper reports on some 20 size distributions of aggregate snowflakes made in the winter of 1951–52.

Data on the size of snowflakes, particularly of a sort useful for radar studies, have lagged behind those for rain; the distribution of raindrops with size, the variation of this distribution with rainfall rate, and the relationship of radar reflectivity to rate of rainfall, have been the subject of study for some time and the reported observations are in generally good agreement (see, for instance, Laws and Parsons, 1943; Marshall and Palmer, 1948; Wexler, 1948; Best, 1950; Blanchard, 1953; Jones, 1956).

Where many of the snow observations that have been reported have dealt with the physical size of the actual snowflakes, the essential need for radar and many other cloud physical studies is a knowledge of the mass of the snow particle. For comparison with rain observations, this is conveniently expressed in terms of the diameter of the water drop to which the snowflake would melt, assuming no break-up. Japanese observers (I. Imai, M. Fujiwara, I. Ichimura, and Y. Toyama, 1955) have recently provided the first size distributions in this form; these covered three periods during a two-hour storm. From these distributions, they have computed the radar reflectivity and the precipitation rate; their data from a single storm fit in well among our data from many storms. Langille and Thain (1951) also provided snow-size distributions in conjunction with radar-signal measurements and their data were further analyzed by Marshall and Gunn (1952), who derived the relation $Z = 200R^{1.6}$. Our present studies lead us to suspect that these data, at least in the latter analysis, and this Z/R relation were incorrect.

The recent Japanese data and those presented here are a cause for some concern when compared with the observed ratio of the radar signal from rain below the bright band (the melting level) to the signal from the snow above the band. Such comparison suggests that there is much to be done in further consideration of processes at the melting level. A considerable contribution to the total rainfall may conceivably be provided by percipitation processes at that level.

2. Sampling technique and reduction of data

A horizontal sheet of brushed angora wool in a shallow box was exposed on the ground in a court sheltered on three sides by buildings. After exposure, the wool was carried inside a warm building; the flakes

[1] The analysis reported in this paper has been sponsored by the Geophysics Research Directorate, Air Force Cambridge Research Center, under Contract AF19(122)–217. The observations were obtained and the data reduced under Project No. 9511–08 of the Defence Research Board of Canada.

melted but did not wet the wool. A filter paper dusted with gentian violet dye was laid on the wool and the drops absorbed. From a previous calibration of the filter paper, the diameter of the drop to which the snowflake melted (or its mass) could be readily measured.

The data from at least 4 filter papers (representing generally about 1000 particles) were reduced to give one distribution. First, frequency histograms were compiled, using 0.2 mm class intervals; a typical one is shown in fig. 1. Then a plot of R_D against D was made (fig. 2), $R_D dD$ being the contribution to the precipitation rate by particles whose melted diameters fell between D and $D+dD$. The quantity R_D for each 0.2-mm interval is given by

$$R_D = \rho \frac{\pi D^3}{6At} \cdot N_h,$$

where ρ is density of water, D is diameter of melted flake, N_h is number of particles per 0.2 mm which fall on filter paper of area A, during exposure time t. This histogram was then smoothed by eye (fig. 2) and the smoothed values of R_D were used to give a smoothed plot of N_H, the number distribution on a horizontal surface (fig. 3). This flux distribution was then converted to a space distribution (N_D against D, fig. 3) using a relationship between fall velocity of aggregate flakes (v) and melted diameter (D) found by Langleben (1954),

$$v = kD^{0.31},$$

where v is in cm sec^{-1} when D is in cm. Langleben found that, at below-freezing temperatures, k ranged from 160 for aggregates of dendrites to 234 for aggregates of plates and columns, and was very sensitive to riming and degree of melting of the flakes. As an average coefficient, $k=200$ was used to convert all the distributions in this series. (Imai *et al* (1955), whose results are discussed in section 5, used $v=207D^{0.31}$ to convert to space distributions.)

Thus the space distribution N_D against D (fig. 3) was obtained from

$$N_D = \frac{N_H}{v},$$

where $N_D dD$ is the number of flakes per unit volume having melted diameters between D and $D+dD$.

The snowfall rate in mm hr^{-1} of melted water was obtained from the area under the histogram of fig. 2.

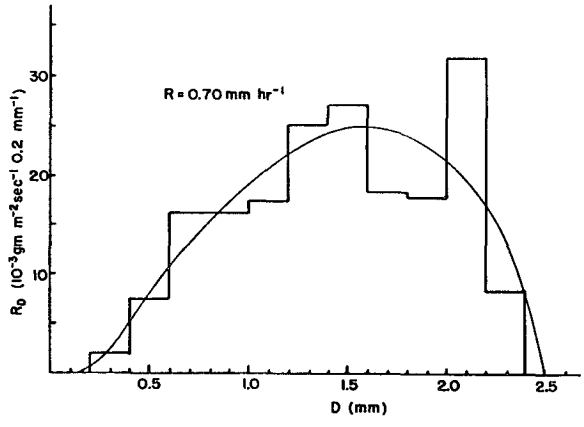

FIG. 2. The histogram of fig. 1 plotted to show the contribution of each 0.2-mm interval to the precipitation rate R. Smooth curve used to compute distributions in fig. 3.

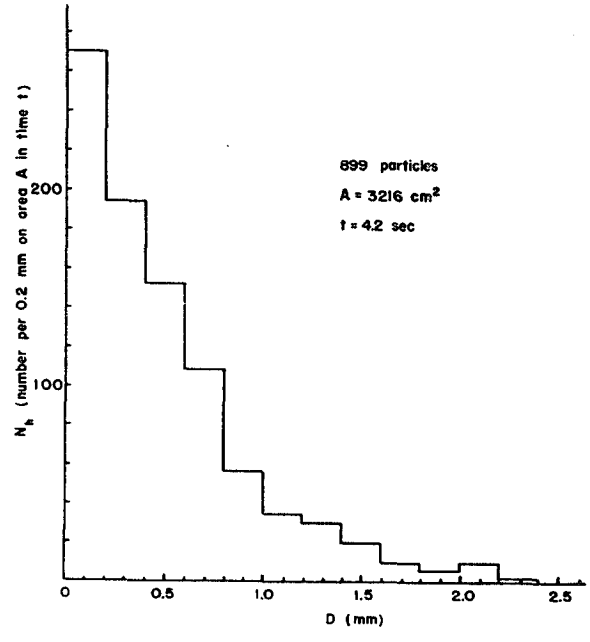

FIG. 1. Frequency histogram of melted particle diameters measured in 0.2-mm intervals from the filter papers. (Sample No. 9 in table 1.)

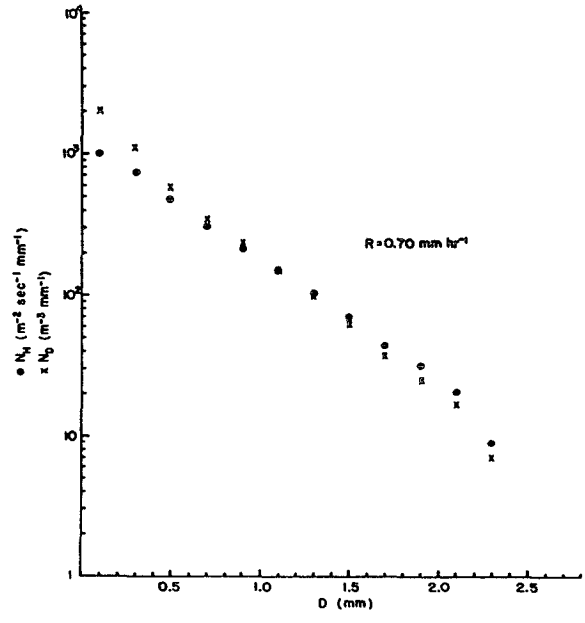

FIG. 3. Smoothed distributions on a horizontal surface (full circles) and in space (crosses). The average relation $v=200\ D^{0.31}$ from Langleben (1954) used to transform from horizontal to space distributions.

Data for 20 distributions taken in the winter of 1951–52 are arranged in table 1 in order of increasing snowfall rate. The snowfalls sampled contained mostly aggregated flakes; on some occasions predominant crystal types were recorded. Temperatures at the ground ranged from −7C to 2C, so that some of the distributions were for snow that had already begun to melt.

3. Average-size distributions

Of the 20 distributions obtained, 15 were used to compile average distributions for four different snowfall rates. (See bracketed samples in table 1.) Each average distribution was obtained by averaging ordinates of the individual distributions at 0.2-mm intervals on a plot of R_D against D (fig. 4). This average distribution was then transferred to coordinates of log N_D against D (points in fig. 5). A straight line of best fit above $D=1$ mm was then drawn through the points on the N_D/D graph, the fit being adjusted slightly to give the correct area (*i.e.*, value of R) on an R_D/D plot (fig. 6). (In addition to this compromise, the final curves in figs. 5 and 6 were slightly adjusted to keep N_0 and Λ simple functions of R).

The four average curves on a plot of log N_D *vs.* D are shown in fig. 5. As found for rain by Marshall and Palmer (1948), the data are fitted well above $D=1$ mm by an exponential of the form

$$N_D = N_0 e^{-\Lambda D}.$$

Unlike the rain distributions, there is not a point of convergence at $D=0$ for all intensities, and N_0 varies with the precipitation rate R. Values of Λ and N_0 for rain and snow are shown in table 2. Also shown are values of median volume diameter D_0; the relation between D_0 and Λ is due to Atlas (1953). Values of R are in millimeters of water per hour. The distribution for a given R for snow is broader than that for rain. At the same time, the range of snowfall rates at the ground is much smaller than rain so that the broadest distribution in snow is about the same as the broadest in rain. This point is illustrated in table 3.

While it has been possible to specify a general form of size distribution which varies systematically with rate of snowfall and so specify a particular value of Λ and N_0 for every value of R, this has only been possible after several samples of snow obtained on different days were averaged. Prior to our attempting such averaging, we were under the impression that the size distribution for snow was much more erratic than rain in its day-to-day variation (fig. 4). This may actually be the case, but it should be borne in mind that the distributions for rain, with which the snow results are compared, are similarly based on averaged data. It is conceivable that the difference between snow and rain is not so much that the snow distributions vary erratically from day to day as that snow data on a given day behave much more consistently than do rain data for a single day.

4. Relations among the parameters Z, R, and M for aggregate flakes

For each of the 20 distributions of table 1, the quantities $Z(=\int_0^\infty N_D D^6 dD)$ and R were computed and a plot made of log Z against log R (fig. 7). A

TABLE 1. Summary of data.

Date	Number of particles (thousands)	Precipitation rate By paper (mm hr^{-1}, melted)	Mean	Screen temp (C)	Ground observations
Mar 6	1.3	0.14		−3.8	columns
Jan 26	1.2	0.22		−2.3	some clusters, some particles rimed
Feb 11	5.9	0.29		−0.7	columns, dendrites some wet clusters
Jan 26	1.8	0.30	0.31	−2.2	some clusters, some particles rimed
Jan 17	2.3	0.33		−7.0	some clusters, some spherical pellets
Jan 26	1.9	0.62		−2.5	some clusters, some particles rimed
Mar 19	1.6	0.67		+1.1	columns, plates
Mar 5	0.9	0.68	0.70	−0.2	rimed dendrites, large clusters
Mar 19	0.9	0.70		+1.0	columns, plates
Nov 3	4.1	0.71		+1.3	columns, plates, some rain
Feb 11	2.0	0.76		+1.6	large clusters
Mar 19	1.8	0.90		+1.2	columns, plates
Jan 26	1.6	1.04		−2.9	some clusters, some particles rimed
Mar 19	2.0	1.09	1.09	+1.2	columns, plates
Mar 19	0.8	1.14		+1.3	columns, plates
Feb 4	2.4	1.28		+0.3	small spherical frozen pellets, some aggregates
Mar 19	1.0	1.65		+1.4	columns, plates
Nov 16	0.8	2.1		+1.5	
Nov 16	0.9	2.5	2.5	+1.8	wet snow, and a few raindrops
Nov 16	1.9	2.8		+2.3	

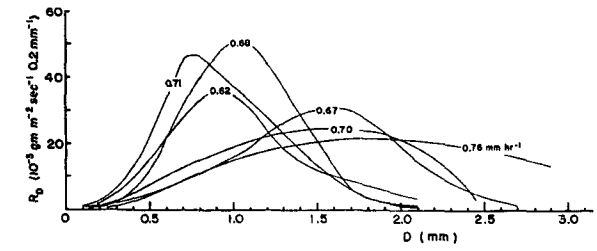

FIG. 4. Six smoothed distributions of R_D against D which were averaged and converted to the distribution in space for $R = 0.70$ mm hr^{-1} in fig. 5.

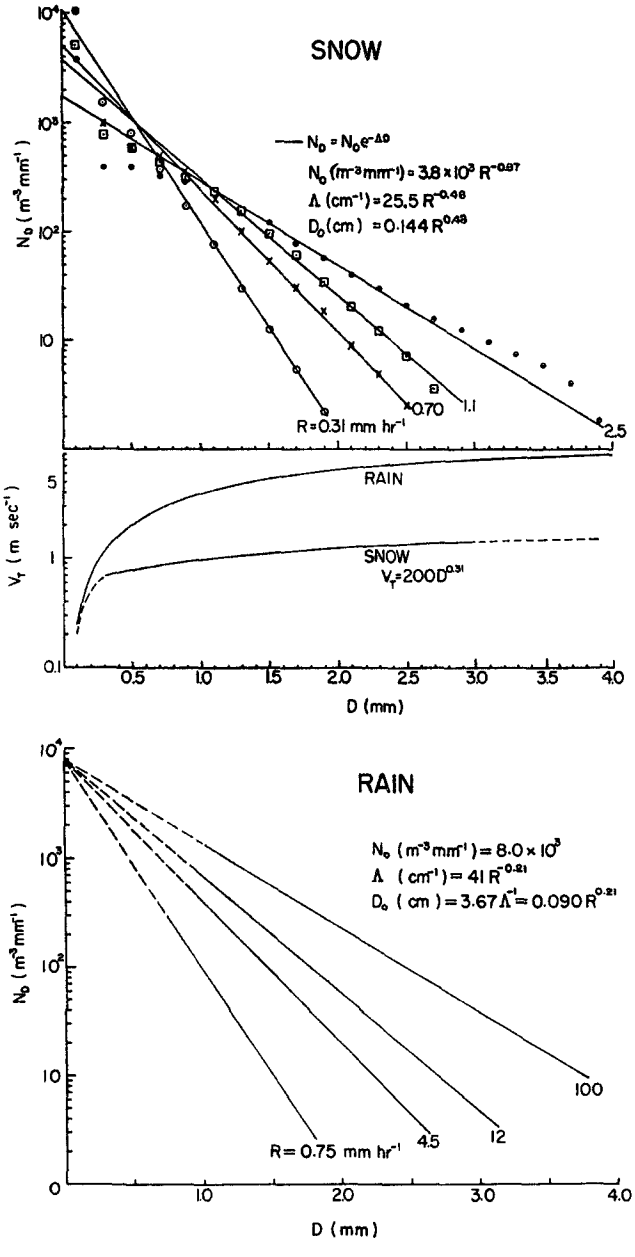

FIG. 5. Top: average distributions in space for aggregate flakes (points) on a plot of log number against melted diameter, fitted by $N_D = N_0 e^{-\Lambda D}$ (solid lines). Middle: terminal speeds of raindrops (from Gunn and Kinzer, 1951) and snowflakes (from Langleben, 1954) as a function of diameter. Bottom: average rain distributions given by Marshall and Palmer's (1948) equation.

locus of best fit, by eye, through the data is $Z = 2000\ R^{2.0}$ with Z in mm^6 m^{-3} and R in mm hr^{-1}. This is an average relation for aggregate snowflakes, and since the distribution for aggregate snowflakes is broader than for rain of a given R, higher Z values are to be expected. Marshall and Palmer (1949), using the same technique of brushed-wool and filter paper, obtained 7 snow distributions. Their data, which included at least two sets for single crystals, are more widely scattered on the Z/R plot, the narrower single-crystal distributions (at $R=1$ and $R=4$ mm hr^{-1}) falling close to the rain locus $Z = 200\ R^{1.6}$. Until these data are added in, the scatter of the Z/R points is of the same order as might be anticipated for a similar number of rain data. The highest R-value among the snow data is only 3 mm hr^{-1}; this value is likely to be exceeded by at least a factor 10 in the case of rain.

The low occurrence of high snowfall rates is not generally appreciated; fig. 8a and 8b have been plotted to illustrate this point. The data consist of two months' snowfall records at McGill (January and February 1954) comprising 300 hours of snow (218 mm melted). From fig. 8b it is apparent that there were only 55 hr (18 per cent of the time) of snowfall greater than 1 mm hr^{-1}, only 10 hr (3.3 per cent) greater than 2 mm hr^{-1}, and only 2 hr (0.7 per cent) greater than 3 mm hr^{-1}. The number of hours in each case might well be multiplied by about 5/3 to be representative of a whole winter's snowfall at Montreal. Thus the probability of observing snow of intensity greater than, for instance, 3 mm hr^{-1} in any one winter is very low.

For each of the 20 distributions, the mass of snow per unit volume (M) was also computed. This was obtained using the plots of R_D *versus* D and computing $M = \int_0^\infty (R_D/v)dD$ where, as before, $v = 200D^{0.31}$ was used. A plot of log M against log R is shown in fig. 9 and a locus of best fit by eye is $M = 250\ R^{0.90}$ with M in mgm m^{-3} and R in mm hr^{-1}. Because the average

TABLE 2. Values of N_0, Λ, and D_0 for rain and snow.

	N_0 (m^{-3} mm^{-1})	Λ (cm^{-1})	D_0 (=3.67 Λ^{-1}) (cm)
Snow	3.8 × 10^3 $R^{-0.87}$	25.5 $R^{-0.48}$	0.144 $R^{0.48}$
Rain	8 × 10^3	41 $R^{-0.21}$	0.090 $R^{0.21}$

TABLE 3. Comparison of Snowfall rate and Rainfall rate.

Snowfall rate (mm hr^{-1})	Λ (cm^{-1})	D_0 (mm)	Rainfall rate for a distribution of same (mm hr^{-1})
0.31	45	0.82	0.75
0.70	30	1.23	4.5
1.1	24.5	1.50	12
2.5	16.5	2.22	100

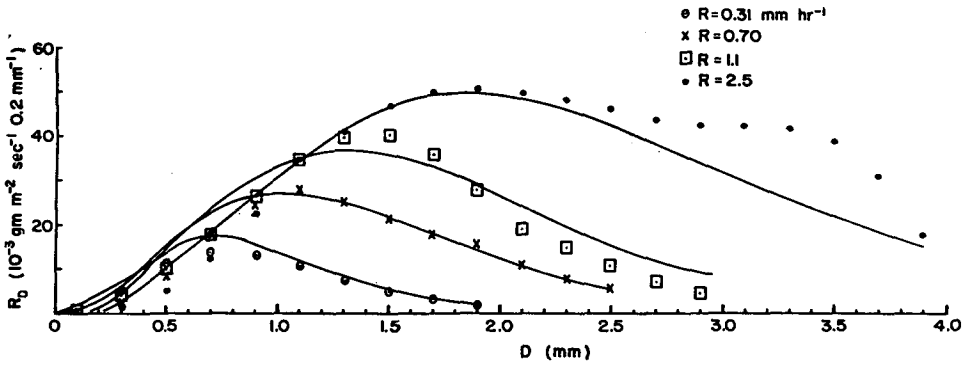

FIG. 6. Showing the fit of the distribution function (solid lines) to the average observed distributions (points) on a plot of R_D *vs.* D.

v that we have used varies only slightly with D, the scatter is small. The index on R is slightly greater than the 0.88 found by Marshall and Palmer (1948) for rain. Had they been identical, the ratio of the effective terminal speeds of rain to snow would be the same for all intensities, namely $250/72=3.5$. As it is, this ratio increases very slightly with increasing R. It might be noted that this ratio is lower than the effective velocity ratio used in converting Z_{snow} to Z_{rain} (section 6) since the peak on a plot of M_D or R_D *vs.* D comes at smaller D's and hence lower v's than on a Z_D *vs.* D plot.

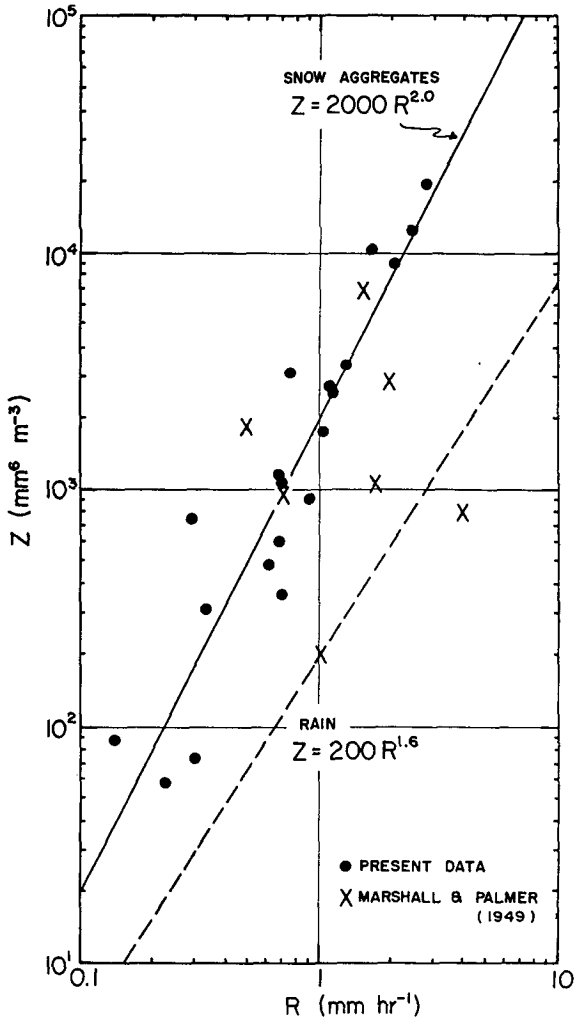

FIG. 7. Log Z plotted against log R for 27 snow samples. The solid line is drawn for best fit by eye through the 20 data of the present study (full circles). The broken line is the Z/R locus for rain revised from Marshall and Palmer (1948).

At $R=1$ mm hr^{-1}, the effective terminal speed for snow, $v(=R/M)$, works out to be 1.11 m sec^{-1}; it varies from 0.8 m sec^{-1} at 0.1 mm hr^{-1} to 1.38 m sec^{-1} at 10 mm hr^{-1}. Workers in the past have often used an effective speed of 1 m sec^{-1} at all R's and thus have not been greatly in error.

On some occasions, at the same time as the samples were being taken on the horizontal angora wool, attempts were made to measure M directly, by sweeping out a known volume of space with a vertical bat covered with angora wool. The values of M measured in this way were a factor 1.5 to 2 lower than those computed from R. Undoubtedly flakes were lost from the vertical wool surface and the values obtained from this method have not been considered.

To obtain the relation between Z and M for aggregate snowflakes, we can combine $Z=2000R^{2.0}$ and $M=250R^{0.90}$ to give $Z=9.57\times10^{-3}M^{2.2}$, where Z is in mm^6 m^{-3} and M in mgm m^{-3}.

5. Comparison with other results

Z/R relationships.—Our sampling involved ten different days extending from 3 November to 19 March, with some subjective avoidance of days with wind and days lacking aggregate flakes. Imai *et al* (1955) measured a comparable number of flakes, all collected within one two-hour period, mostly within the range $R=0.1$ to $R=1$ mm hr^{-1}. During the first 20 min there was a relative scarcity of aggregate flakes, as evidenced by photographs and size distributions, and the Z/R data fell about the regression line $Z=600R^{1.8}$. There was then a sudden change, and all subsequent points fall close to the line $Z=2150R^{1.8}$. The departure during the first twenty minutes toward

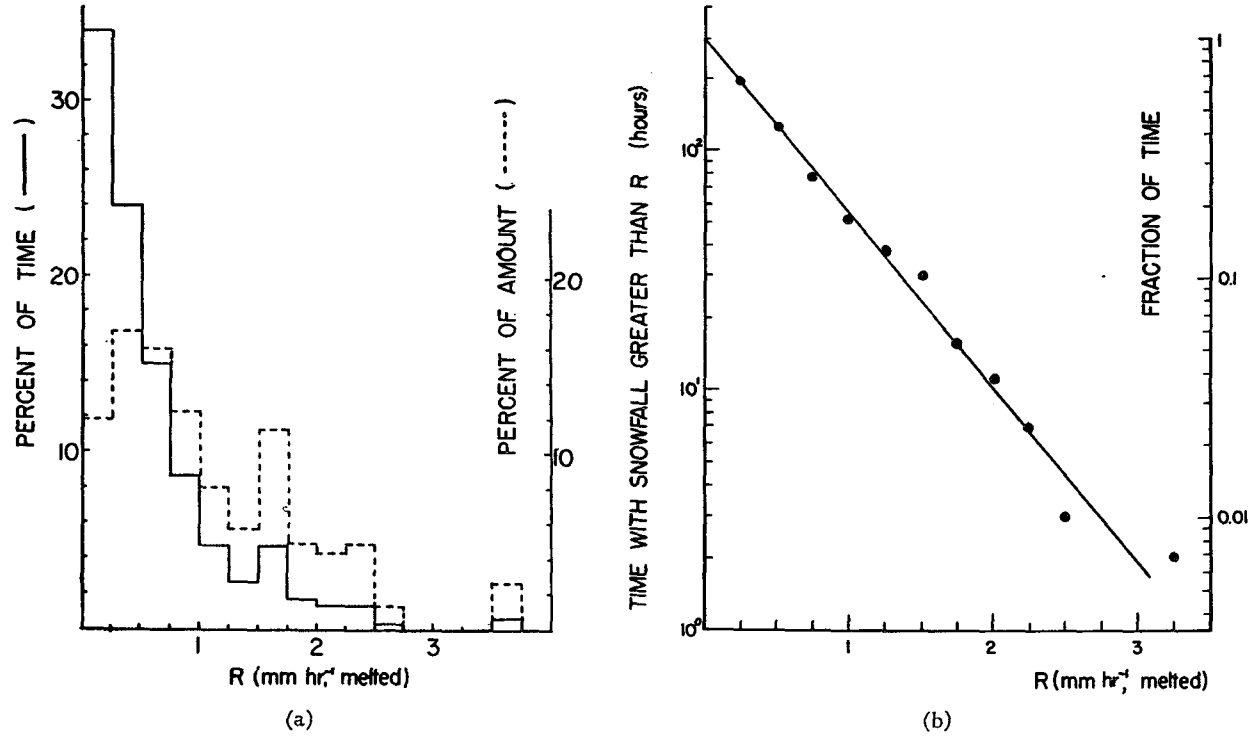

FIG. 8a (left). Distribution of number of hours of snowfall and total amount with snowfall rate (R) at Montreal, January and February 1954. b (right). The number of hours of snowfall with R greater than a given value falls off exponentially with increasing R.

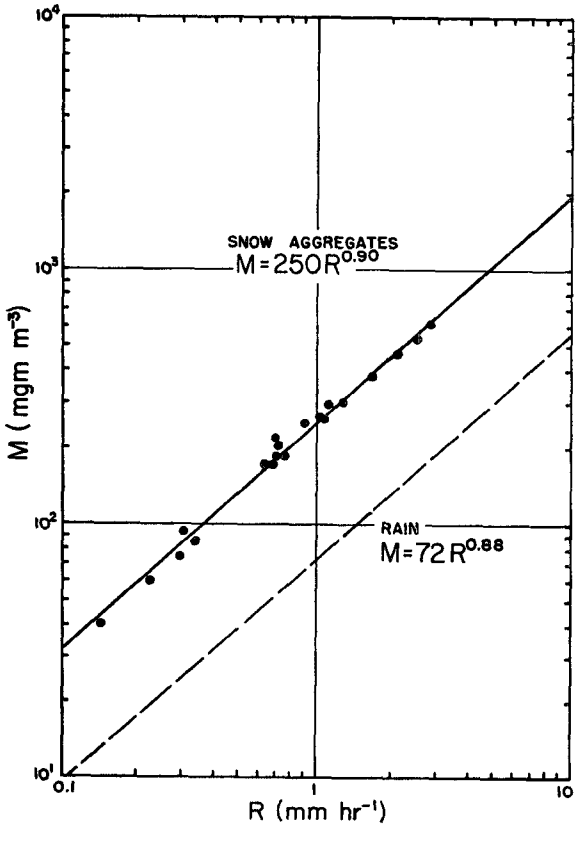

FIG. 9. Log M plotted against log R for 20 snow samples. The solid line is drawn for best fit by eye. The broken line is the M/R locus for rain (Marshall and Palmer, 1948).

lower Z for a given R, like two points of Marshall and Palmer's is very likely attributable to predominance of single crystals in the samples, a situation that we appear to have avoided in the present work.

The most notable disagreement is with work previously reported by ourselves (Marshall and Gunn, 1952). At that time, observations made by Langille and Thain (1951) were analyzed to reveal a broad scatter of Z/R data about $Z=200R^{1.6}$. The present locus $Z=2000R^{2.0}$ fits the older data quite well as an an upper boundary, while the lowest Z values for any R in those data were far lower than for any other available data. The method of analysis involved in this earlier work was indirect, but a careful review has revealed no error in it. It is worth noting, however, that the samples were caught directly on the filter paper on which they were subsequently melted. Even on brushed wool, there is a tendency for aggregate flakes to break up into individual crystals and on the relatively hard surface of filter paper these crystals are bound to bounce and wander. Langille and Thain, with their lower temperatures and stronger winds, may have been less successful than Imai *et al* in keeping track of the array of crystals belonging to a single aggregate. Langille and Thain deserve credit for their measurements of R, which were derived from samples collected on a large ground-sheet over five-minute periods. In dealing with rain, it is found preferable to take R from a rain-gauge rather than

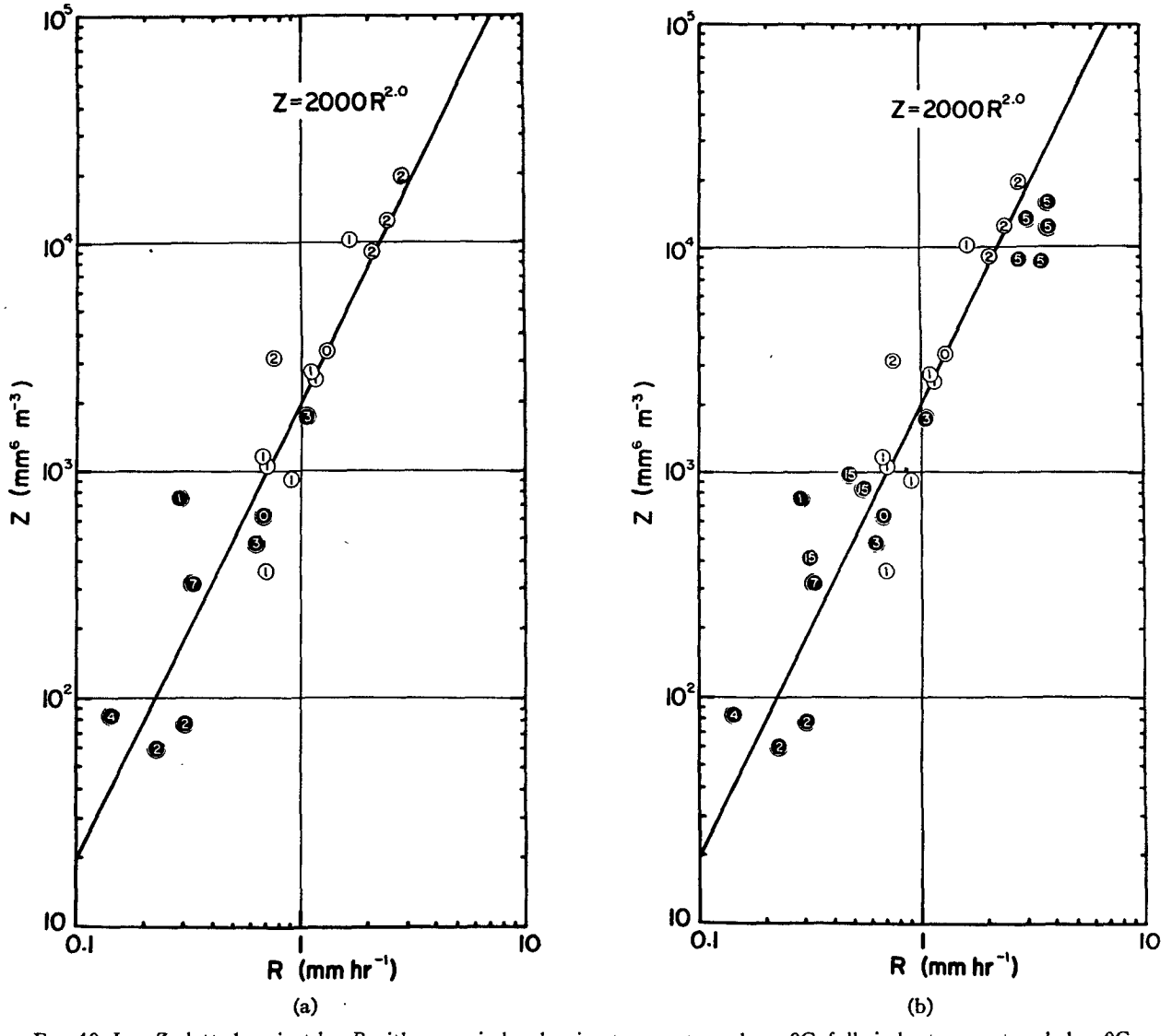

FIG. 10. Log Z plotted against log R with open circles showing temperature above 0C, full circles temperature below 0C; (a) with original data, (b) with eight additional low temperature points added.

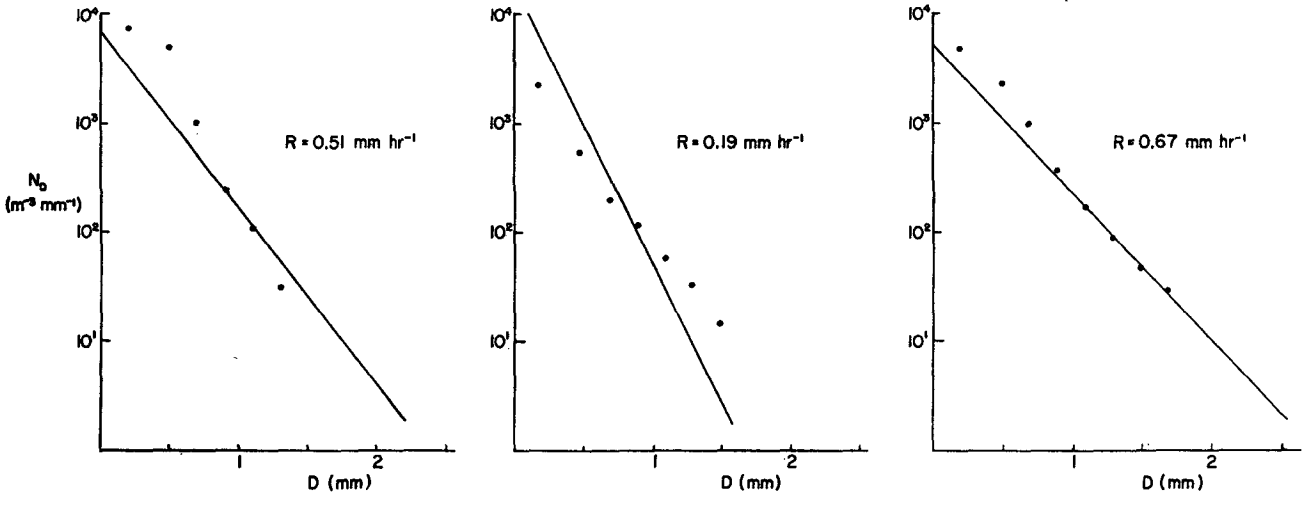

FIG. 11. Three average size distributions for snow (full circles) from Imai *et al* (1955), compared with average snow distributions $N_D = N_0 e^{-\Lambda D}$ for the same intensity (straight lines).

from the filter-paper samples. It seems reasonable, therefore, to attempt some similarly independent measurement of R in the case of snow, though in the Japanese observations and in the work reported here R was computed from the filter papers.

In the course of analyzing the Z/R data of fig. 7, a disconcerting temperature trend was observed. The data are replotted in fig. 10a to show this. Open circles give ground temperatures above OC; full circles, temperatures below OC. The air temperature at the ground apparently increases with the observed rate of snowfall; most of the data for $R>1$ mm hr^{-1} are for ground temperatures a degree or two above OC. A check through two months' snowfall records (January and February 1954) showed no evidence to back up this trend. Nevertheless, we delayed submission of these results until some further low-temperature observations had been made. In fig. 10b, eight points (five at -5C, three at -15C) observed in February 1957 have been added. The added data confirm that the temperature trend was probably a coincidence and they do not call for any significant change in the locus $Z=2000R^2$.

Size distributions.—Imai *et al* (1955), who sampled the snowflakes continuously during their two hours of observation, presented three distributions characteristic of each of three periods in those two hours. Each distribution was averaged over a period of some 7 to 12 min. Their distributions, plotted as N_D against D, were for the rain to which the snow would melt and so involved the terminal speed of raindrops. We have converted these distributions, using $v=200\ D^{0.31}$ for snowflake terminal speeds, back to snow and plotted them with our average distribution for the same R (fig. 11). The distributions at $R=0.67$ mm hr^{-1} fit best, but considering that ours are the average of data taken on many occasions, the agreement of all three is good.

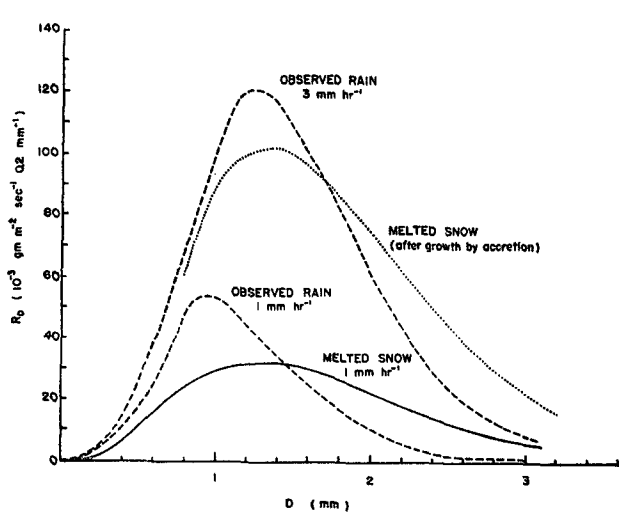

FIG. 12. Average distributions with diameter (melted diameter in the case of snow) for aggregate snowflakes (solid line) and for rain (broken lines). Dotted line gives distribution for snow that has grown to 3 mm hr^{-1} from 1 mm hr^{-1} by accretion of cloud.

They compared their melted snow distributions for the three periods with the Marshall and Palmer (1948) average rain distributions and there was reasonably good agreement. Similarly good fits can be obtained by treating our snow distributions in the same way at these low intensities. However, beyond about $D=2$ mm, the rain and snow velocities (fig. 5) maintain an almost constant ratio and the change in Λ resulting from melting is negligible. As a result, our distributions at 1.1 and 2.5 mm hr^{-1}, when melted to rain, are much broader than the observed rain distributions for the same R.

6. Rain formed from melted snow

Comparison of snow and rain distributions.—The solid-line curve of fig. 12 gives the distribution of snowfall arriving at the ground with particle size (specifically the diameter of a sphere of water of the same mass) for a precipitation rate of 1 mm hr^{-1}. If the snow were to melt, with each snowflake changing to a single raindrop of the same mass, this distribution would be the same for the melted snow as for the snow.

For comparison, the broken line labelled 1 mm hr^{-1} gives the average observed distribution for rainfall, based on Marshall and Palmer's (1948) *data*. This is effectively a smooth curve drawn through the data, and the area under it is 1 mm hr^{-1}. A similar curve based on Marshall and Palmer's *equation* would have more small-drop rain, and the area under it would be greater than 1 mm hr^{-1}. The corresponding discrepancy between equation and data is negligible in the case of the snow distributions.

Comparing the distribution for snow or melted snow with that for rain of the same intensity, it can be seen that the "melted snow" contains more big drops than the observed rain. Thus for 1 mm hr^{-1} of snow to change to rain of the same intensity, and with the distribution observed for rain, it would be necessary that the larger flakes come apart on melting to form several smaller raindrops.

In relating snow-to-rain distributions, it is useful to bear in mind an indication from radar data (discussed in the next section) that the intensity of precipitation increases on melting. The significant change then is not from 1 mm hr^{-1} of snow to 1 mm hr^{-1} of rain but more appropriately from 1 mm hr^{-1} of snow to 3 mm hr^{-1} of rain. Therefore, fig. 12 also includes the observed distribution for 3 mm hr^{-1} of rain which is seen to fall everywhere above the 1 mm hr^{-1} of snow.

We have calculated the growth by accretion that would be required to take the 1 mm hr^{-1} melted snow to the order of 3 mm hr^{-1} rain. Neglecting updraft, it requires the disconcerting fall distance of 15,000 ft

through cloud of 0.2 gm m^{-3} (assuming 100 per cent collection efficiency). The resulting curve (dotted) still seems to require some break-up for its conversion to the observed-rain distribution.

The time for break-up, of course, is upon melting, prior to growth. A moderate amount of break-up at that stage would not only avoid the large particle excess in the dotted curve but it would also reduce the required fall distance significantly, especially when updraft was taken into account.

Comparison of radar signals.—The relationships between Z and R for snow aggregates and for rain were compared in fig. 7. Modified forms of this Z/R plot can help in the comparison. In fig. 13a, the full circles representing the snow data, and their locus, have been lowered by a factor 5.4. This is approximately the ratio of the terminal speed of a raindrop to that of a snowflake of the same mass for all sizes contributing significantly to Z. Thus the full circles in fig. 13a are appropriate to melted snow, on the assumption that each snowflake melts to a single raindrop. The more numerous smaller dots with the broken line through them are the earlier rain observations, for comparison. The departure of "melted snow" from observed rain, increasing with R, can be seen.

The intensity of radiation scattered by a precipitation particle is proportional to $S|K|^2Z$, where S is a shape factor and $|K|^2$ a dielectric factor. The factor S is unity for a sphere and increases with any distortion from that shape, the increase depending on the extent of the distortion and the nature of the dielectric. The factor is not likely to be more than 1.25 for dry snow, and will be somewhat above unity for rain; here it will be taken equal to unity for both rain and snow.

The ordinate of fig. 13b then is a measure of radar

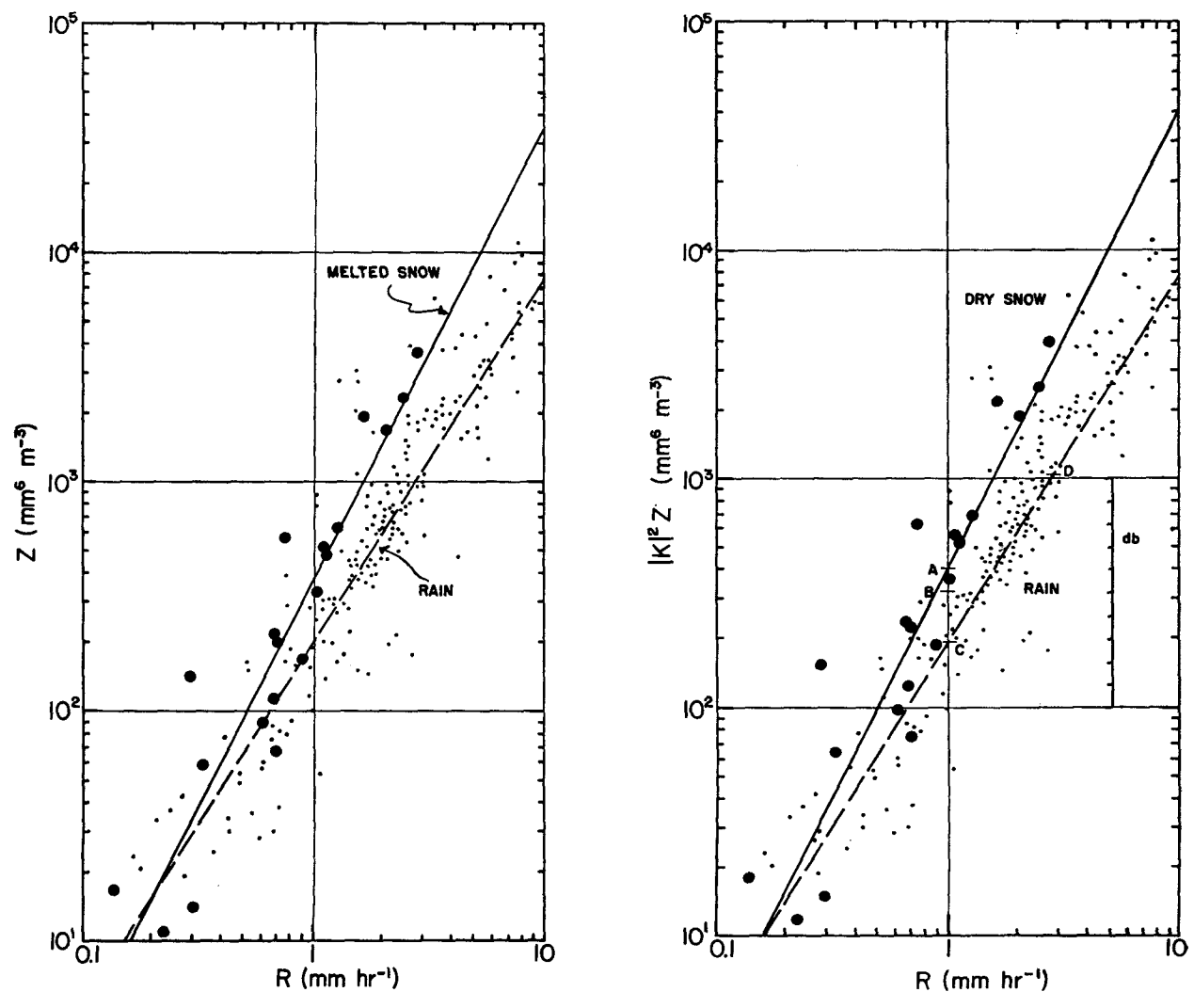

(a) (b)

FIG. 13. (a) Rain data (small dots) and melted snow data (full circles), assuming each snowflake melts to a single raindrop, on a plot of log Z against log R. (b) The radar signal (proportional to $|K|^2Z$) from dry snow (full circles) is on the average greater than the signal from rain (dots) at any R. After melting, the snow locus would pass through point B.

reflectivity. For a precipitation rate of 0.16 mm hr^{-1}, snow and rain give the same radar signal; at 1 mm hr^{-1} the signal from rain is 3 db weaker than from snow; at 3 mm hr^{-1}, 5 db weaker. This is contrary to radar observations (Austin and Bemis, 1950; Hooper and Kippax, 1950; Mason, 1955) which show the signal from the rain to be anywhere from 2 db weaker to 10 db stronger than from the snow, or 4 db stronger on an average. Growth of precipitation at the melting level would seem the only way that the radar and size distribution evidence can be made to agree.

Starting with snow at 1 mm hr^{-1} (point A), the requirement is to rise to a signal stronger by 4 db from rain. This takes us to the point *D*. Now, melting without any break-up reduces the signal from *A* to *B* (for melted snow). Break-up would reduce the signal further, to the point *C*, which we have put rather arbitrarily on the rain locus. Then growth by accretion as considered above would increase both *R* and the signal strength to reach the point *D*.

The possible growth processes that have been barely mentioned here have been discussed in detail elsewhere (Atlas, 1955; Wexler and Atlas, 1956). Essentially, melting snow at the melting level chills the saturated air. This may not only permit growth by condensation but can lead to the cloud required for subsequent accretion. It may still be very difficult, however, to explain quantitatively as great an increase in *R* at the melting level as the radar observations suggest.

Acknowledgments.—The authors wish to acknowledge the assistance of Mrs. M. W. M. Smith (Miss E. C. Rigby) and Dr. M. P. Langleben on the many occasions of snow sampling.

REFERENCES

Atlas, D., 1953: Optical extinction by rainfall. *J. Meteor.*, **10**, 486–488.

——, 1955: *The radar measurement of precipitation growth.* Mass. Inst. Tech. Sc.D. Dissert. 239 pp.

Austin, P. M., and A. C. Bemis, 1950: A quantitative study of the "bright band" in radar precipitation echoes. *J. Meteor.*, **7**, 145–151.

Best, A. C., 1950: The size distribution of raindrops. *Quart. J. r. meteor. Soc.*, **76**, 16.

Blanchard, D., 1953: Raindrop size-distribution in Hawaiian rains. *J. Meteor.*, **10**, 457.

Gunn, R., and G. D. Kinzer, 1949: The terminal velocity of fall for water droplets in stagnant air. *J. Meteor.*, **6**, 243–248.

Hooper, J. E. N., and A. A. Kippax, 1950: The bright band, a phenomenon associated with radar echoes from falling rain. *Quart. J. r. meteor. Soc.*, **76**, 125–132.

Imai, I., M. Fujiwara, I. Ichimura, and Y. Toyama, 1955: Radar reflectivity of falling snow. *Pap. in Meteor. and Geophys. (Japan)*, **6**, 130–139.

Jones, D. M. A., 1956: *Rainfall drop size-distribution and radar reflectivity.* Res. Rep. No. 6, Signal Corps Proj. 172B, Illinois State Water Survey, 20 pp.

Langille, R. C., and R. S. Thain, 1951: Some quantitative measurements of three centimeter radar echoes from falling snow. *Canadian J. Phys.*, **29**, 482.

Langleben, M. P., 1954: The terminal velocity of snow aggregates. *Quart. J. r. meteor. Soc.*, **80**, 174–181.

Laws, J. O., and D. A. Parsons, 1943: The relation of drop-size to intensity. *Trans. Amer. Geophys. Union*, **24**, II, 452–459.

Marshall, J. S., and K. L. S. Gunn, 1952: Measurement of snow parameters by radar. *J. Meteor.*, **9**, 322.

——, and W. McK. Palmer, 1948: The distribution of raindrops with size. *J. Meteor.*, **5**, 165–166.

——, and ——, 1949: *Rain and snow distributions.* Pap. read at the annual meeting of the R. Soc. of Canada.

Mason, B. J., 1955: Radar evidence for aggregation and orientation of melting snowflakes. *Quart. J. r. meteor. Soc.*, **81**, 262–264.

Wexler, R., 1948: Rain intensities by radar, *J. Meteor.*, **5**, 171–173.

——, and D. Atlas, 1956: Factors influencing radar-echo intensities in the melting layer. *Quart. J. r. meteor. Soc.*, **82**, 349–352.